INSTITUTE OF PHYSICS PUBLISHING NANOTECHNOLOGY
Nanotechnology **13** (2002) 258–262 PII: S0957-4484(02)31003-1

A tunnelling spectroscopy study on the single-particle energy levels and electron–electron interactions in CdSe quantum dots

E P A M Bakkers[1,2], Z Hens[1], L P Kouwenhoven[3], L Gurevich[3] and D Vanmaekelbergh[1]

[1] Debye Institute, University of Utrecht, PO Box 80000, 3508 TA Utrecht, The Netherlands
[2] Philips Research, Prof. Holstlaan 4, 5656 AA Eindhoven, The Netherlands
[3] Department of Applied Physics and ERATO Mesoscopic Correlation Project, Delft University of Technology, PO Box 5046, 5600 GA Delft, The Netherlands

E-mail: erik.bakkers@philips.com

Received 20 November 2001, in final form 18 February 2002
Published 9 May 2002
Online at stacks.iop.org/Nano/13/258

Abstract
We performed scanning tunnelling spectroscopy on insulating colloidal CdSe quantum dots attached to gold with a rigid self-assembled monolayer. By varying the tip–dot distance we change the relative rate of tunnelling into versus tunnelling out of the dot over a wide range. If the tip is retracted relatively far from the dot, tunnelling in is much slower than tunnelling out of the dot; electrons tunnel one at a time through the dot. The resonances in the conductance spectrum correspond to the single-particle energy levels of the CdSe quantum dot. When the tip is brought closer to the dot, tunnelling in can become as fast as tunnelling out of the dot. Up to three electrons can be present in the particle; the electron–electron Coulomb interactions lead to a more complex conductance spectrum.

1. Introduction

Insulating crystals with dimensions in the nanometre regime might play an important role in bottom-up electrical nanodevices. The large level spacing and the extremely small capacitance of these quantized semiconductor dots make them suitable candidates as active centres in room-temperature single-electron transistors [1, 2]. Even a very small difference of the gate voltage (0.1–0.3 V) can switch the current from off to on; this is in contrast to conventional field effect transistors, where higher gate potentials must be applied (5–10 V).

Control of the size, shape and surface chemistry of colloidal quantum dots has greatly improved during the last decade [3]. A critical step, however, is the implementation of particles in devices to form logic gates. Positioning of the dots at specific places on a surface or in a network and contacting them individually in a reproducible way is still complicated. Colloidal particles can be attached to a surface using a self-assembled monolayer of organic spacer molecules [4]. Although this method is not site selective, it gives us the opportunity to vary the distance, and thus to tune the tunnel barrier between the quantum dot and a metal electrode. The significance of the tunnel barriers on the performance of a single-electron device has been shown by Su *et al* [5].

Another issue is the electronic structure of semiconductor particles. Pseudopotential and tight-binding methods have been used to calculate the single-particle energy level spectrum of a number of nearly spherical nanocrystals, such as InAs and InP [6, 7], CdSe [8], Ge [9] and Si [10] nanocrystals. Experimentally, the electronic structure of colloidal nanocrystals can be studied with both optical and electronic methods. With optical techniques only the energy differences between valence band and conduction band states are obtained. It has proven to be very difficult to assign all optical transitions and to derive the energy level spectrum from optical data [11, 12]. The advantage of electronic methods is that the absolute position of the electron energy levels and electron–electron interactions can be probed directly [13].

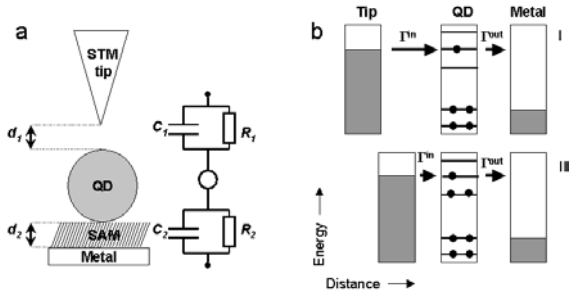

Figure 1. (*a*) A DBTJ is formed when an STM tip is placed above the quantum dot. The distance between the dot and the substrate, d_2, is fixed by the SAM. The distance between the dot and the tip, d_1, is adjusted by the STM settings. (*b*I) *Shell-tunnelling spectroscopy.* The tip is retracted from the dot, such that tunnelling from the tip into the dot is much slower than tunnelling from the dot to the substrate: electrons tunnel one at a time through the device; electron–electron interactions do not occur. (*b*II) *Shell-filling spectroscopy.* The tip is brought close to the dot, such that tunnelling from the tip into the dot is much faster than tunnelling out of the dot. Electronic orbitals are multiply occupied, and the degeneracy of the states is lifted by electron–electron Coulomb interactions.

A versatile way to investigate both the transparency of the tunnel barriers and the electronic structure of colloidal quantum dots is provided by scanning tunnelling spectroscopy [14]. The colloidal crystals are attached to a conducting substrate. A double-barrier tunnel junction (DBTJ) is formed by locating an STM tip above a nanocrystal as illustrated in figure 1(*a*). The tunnel current I is monitored as a function of the bias V, which is the difference in the electrochemical potentials of the tip and substrate electrode: $\mathrm{eV} = \mu_{\mathrm{e}}^{tip} - \mu_{\mathrm{e}}^{substrate}$. If the applied bias is such that μ_{e}^{tip} is in resonance with the first discrete electron level of the quantum dot, tunnelling from the tip to this level can occur, followed by tunnelling to the substrate. This results in an increase of the current, i.e. a step in the (I, V) plot, and, hence, a peak in the $\partial I/\partial V$ versus V relationship (conductance or tunnelling spectrum). A second peak in the tunnelling spectrum will be found when μ_{e}^{tip} comes in resonance with the second electron orbital, etc.

There are two important effects which should be considered for a valid interpretation of resonant tunnelling spectra. First, the interpretation of tunnelling spectra is simplified if the electrochemical potential (Fermi level) of one of the electrodes remains constant with respect to the energy levels of the quantum dot, while the electrochemical potential of the other electrode changes equally with the bias V. With an STM, such an asymmetrical distribution of the bias over both tunnelling barriers can be achieved, in principle, by retracting the tip sufficiently far from the dot, such that $C_1 \ll C_2$. It is, however, difficult to reach a completely asymmetrical distribution [15].

Second, electron–electron Coulomb interactions in the quantum dot may have a profound effect on the tunnelling spectra. The probability that these interactions occur is determined by the dynamics of electron tunnelling into and out of the quantum dot [5, 16]. If we consider tip-to-dot-to-substrate tunnelling (at $V > 0$), the probability of finding an electron in the LUMO of the quantum dot (an s-type orbital) is given by

$$P[\mathrm{s}^1] = \frac{\Gamma_{\mathrm{s}}^{in}}{\Gamma_{\mathrm{s}}^{in} + \Gamma_{\mathrm{s}}^{out}}, \tag{1}$$

in which Γ_{s}^{in} is the electron tunnelling rate for tunnelling from the tip into the empty s orbital, and $\Gamma_{\mathrm{s}}^{out}$ that for tunnelling from the s orbital into the substrate electrode. We first consider the case in which $\Gamma_{\mathrm{s}}^{in} \ll \Gamma_{\mathrm{s}}^{out}$. Hence, one electron tunnels at a time through the nanodevice, and the quantum dot never contains more than one additional electron. Thus, tunnelling leads to charging of the dot by a single electron (i.e. dielectric solvation [17]), although Coulomb interactions between two (or more) additional electrons do not occur. This still holds when the electrochemical potential of the tip electrode is increased, such that tunnelling from the tip to the second level (a p-type level) also occurs. In this type of spectroscopy, i.e. shell-tunnelling spectroscopy [14], electron–electron Coulomb interactions do not occur; this means that the peaks in the conductance spectrum correspond to the single-particle orbital energy spectrum. In contrast, in the case where $\Gamma_{\mathrm{s}}^{in} \gg \Gamma_{\mathrm{s}}^{out}$, the s orbital will be occupied with one electron at the first resonance ($P[\mathrm{s}^1] \cong 1$). When μ_{e}^{tip} is further increased, a second resonance will be met, corresponding to the filling of the s orbital with a second electron. Then, the energy difference between the first and second resonances corresponds to the electron–electron Coulomb energy in the s orbital. The third resonance corresponds to the occupation of a p orbital with one electron while the s orbital is doubly occupied. Thus, shell-filling spectroscopy [14] corresponds to a more complex spectrum, in which the degeneracy of the orbitals is lifted due to electron–electron Coulomb interactions. Recently, shell-filling spectra of InAs quantum dots have been presented, showing that the first electron orbital (LUMO) is an s-type double-degenerate orbital, and the second orbital is a sixfold-degenerate p-type orbital [18, 19].

In this paper, we demonstrate that electron–electron Coulomb interactions can effectively be turned on and off by controlling the tunnelling dynamics in the substrate/quantum dot/tip device. We vary the width of the dot–tip tunnelling barrier, d_1, and show that the relative rate of tip-to-dot and dot-to-substrate tunnelling critically determines the electron occupation in the CdSe quantum dot (see figure 1(*b*)). If the tip is sufficiently retracted, electrons tunnel one at a time through the tip/Q-CdSe/spacer/Au device; the shell-tunnelling spectrum obtained corresponds to the single-electron energy level spectrum. We show that the spectra become more complex when the tip is brought closer to the dot. The peaks in the tunnelling spectra can, however, be assigned with the aid of Monte Carlo simulations of the electron occupation in the CdSe quantum dot. As a result, the electron–electron interaction energy can be distinguished from the single-particle energy separations between the orbitals.

2. Experiment

Colloidal TOP/TOPO capped CdSe nanocrystals with a diameter of 43 Å were prepared according to [20]. The gold samples were flame annealed and provided with a SAM of sulfur-terminated oligo(cyclohexylidene) molecules. A sub-monolayer of quantum dots was deposited on the SAM by placing the sample in a CdSe suspension. In this way,

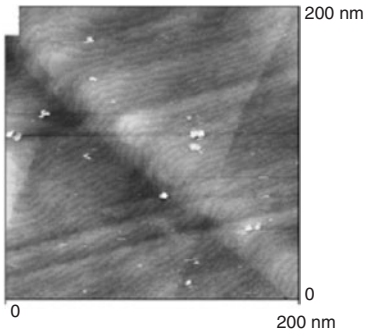

Figure 2. STM image of a sub-monolayer of CdSe particles on a Au(111) surface covered with a SAM of sulfur-terminated oligo(cyclohexylidene) molecules.

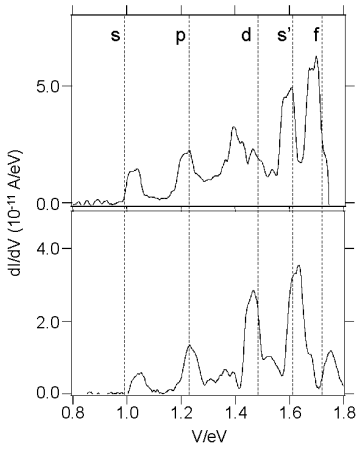

Figure 3. Part of the tunnelling spectra of two 43 Å CdSe quantum dots taken at a relatively large tip–dot distance at 4.2 K (setpoint 5×10^{-12} A at 1.4 eV, estimated tip–dot distance 14 Å, see text). The dotted lines correspond to the electron orbitals according to pseudo-potential theory.

the dot/substrate distance, d_2, is set at 8 Å [21]. STM measurements at 4.2 K were performed on a home-built STM in a vacuum chamber containing a small amount of helium. For tunnelling spectroscopy the tip was positioned above an individual quantum dot and the tunnelling and feedback controls were switched off. The conductance spectra were obtained by numerically differentiating the measured I–V curves.

3. Results

Figure 2 shows a topographic STM image of the sub-monolayer of CdSe nanocrystals on the Au(111) surface covered with a SAM. Tunnelling spectra were recorded on isolated quantum dots.

In figure 3, parts of typical conductance spectra are presented for two 43 Å CdSe quantum dots under conditions where the tip is retracted relatively far from the dot (see figure caption). A zero conductivity gap was found between 1 and −1.6 eV bias. Negative of −1.6 eV, several small conductance peaks were observed corresponding to tunnelling through the first valence band orbitals (hole states) of the CdSe quantum dot. In the bias range more positive than 1 eV, five peaks are observed, increasing in height with increasing energy. The tunnelling spectra become unstable at a bias exceeding 1.8 eV. Tunnelling spectra acquired with comparable CdSe quantum dots under the same conditions show the same features. We infer that the spectrum shown in figure 3 is a shell-tunnelling spectrum; this will be validated by the analysis given below. The results obtained with shell-tunnelling spectroscopy were compared with the energy level spectrum obtained from a pseudo-potential calculation in figure 3. The pseudo-potential calculation was performed for a facetted and capped CdSe quantum dot with an approximately spherical shape; the model quantum dot that comes closest to the experimentally investigated dots has a diameter of 47 Å. The first conductance peak at negative bias corresponds to tunnelling of a hole through the HOMO, the first peak at positive bias in figure 3 to tunnelling of an electron through the LUMO. The zero-conductivity gap thus corresponds to the quasi-particle gap of the quantum dot, i.e. the LUMO–HOMO single-particle gap plus the self-polarization energies (charging energies) due to either an electron in the LUMO or a hole in the HOMO. Pseudopotential theory predicts a value of 2.21 eV for the LUMO-HOMO single-particle gap for the model CdSe quantum dot. The self-polarization energies of the incoming electron and hole depend sensitively on the effective dielectric constant of the immediate environment of the quantum dot [17]. For an effective dielectric constant of 2, pseudo-potential theory predicts a value of 0.147 and 0.125 eV for the single-electron and single-hole charging energy, respectively. This amounts to a quasi-particle gap of 2.48 eV. There is a good agreement between the experimental values (average value 2.44 eV) and that predicted with pseudo-potential theory of 2 for the effective dielectric constant of the environment. Furthermore, the optical bandgap of the 4.3 nm CdSe colloids is 2.15 ± 0.05 eV, as determined from the first peak in the absorption spectrum. We determine the electron–hole Coulomb energy from the difference between the quasiparticle gap and the optical gap, and find a value of 0.29 eV, in excellent agreement with the pseudo-potential value (also 0.29 eV) predicted for the model dot imbedded in a dielectric with a dielectric constant of 2.

The conductance peaks observed at negative bias correspond to tunnelling through the HOMO and other valence band orbitals. The peaks are closely spaced in energy, in qualitative agreement with the theoretical prediction. The peaks are, however, not well resolved and do not allow a more quantitative analysis. The peaks at positive bias correspond to tunnelling through the electron orbitals of the CdSe dot, s, p, d, s′ and f type in order of increasing energy [14]. The current steps increase in height with increasing energy, reflecting the increasing spatial extension of the orbitals. The first peak occurs at $\mu_e[s^0p^0/s^1p^0] = \varepsilon_s + \Sigma_s$, the second peak at $\mu_e[s^0p^0/s^0p^1] = \varepsilon_p + \Sigma_p$, where Σ_s (Σ_p) is the polarization energy of an electron in the s orbital (p orbital). Thus, the energy difference between the second and first peaks is given by $(\varepsilon_p - \varepsilon_s) + (\Sigma_p - \Sigma_s)$. It follows from pseudo-potential calculations that the difference between the self-polarization energies of electrons in p and s orbitals, $\Sigma_p - \Sigma_s$, does not exceed $(\varepsilon_p - \varepsilon_s)/10$. Hence, we conclude that the energy difference between the second and first peaks should be approximately equal to $\varepsilon_p - \varepsilon_s$, the difference between

the single-electron orbital energies. Similarly, the energy differences between the third and second, fourth and third and fifth and fourth peaks should be approximately equal to $\varepsilon_d - \varepsilon_p$, $\varepsilon_{s'} - \varepsilon_d$ and $\varepsilon_f - \varepsilon_{s'}$, respectively. The experimentally observed energy separations, which should be corrected for $\Delta\mu_e^{tip}/V = 0.9$, can be compared with the pseudo-potential calculations. It can be seen in figure 3 that the experimental separations between the second and first and between the third and second are, on average, 75% of the pseudo-potential values for $\varepsilon_p - \varepsilon_s$ and $\varepsilon_d - \varepsilon_p$ respectively. The experimental separations between the fourth and third and fifth and fourth peaks are in good agreement with the predicted values of $\varepsilon_{s'} - \varepsilon_d$ and $\varepsilon_f - \varepsilon_{s'}$, respectively. It is not yet clear why the observed energy separations between $\varepsilon_p - \varepsilon_s$ and $\varepsilon_d - \varepsilon_p$ are significantly smaller than predicted by pseudo-potential theory. We remark here that a number of experimental uncertainties exist. The first one is related to the size distribution of the CdSe nanocrystals (43 Å ± 10%), leading to ±20% uncertainties in the energy differences between the energy levels. A second one is related to the shape: it is not possible to detect small deviations from a spherical shape *in situ* with STM.

The conductance spectra change gradually when the tip is brought closer to the CdSe quantum dot. Figure 4 shows a typical spectrum in the positive bias range, obtained with a 12 times higher setpoint current than used to acquire the shell-tunnelling spectrum in figure 3. Under these conditions we first find three closely spaced peaks, decreasing in intensity. There is also some additional structure (i.e. small satellites) close to peaks E. The occurrence of closely spaced peaks indicates the breakdown of the spin and orbital degeneracy due to electron–electron Coulomb interactions in the quantum CdSe dot. In other words, more than one electron tunnels at a time through the device. This is confirmed by results acquired at even smaller tip–dot distances (larger setpoint currents) showing a large number of closely spaced peaks.

We simulated the (I, V) tunnelling spectra of CdSe quantum dots using a Monte Carlo algorithm [22]. The energy scheme for the single-particle orbitals, obtained from pseudo-potential theory for a CdSe nanocrystal with a diameter of 47 Å, was used as input; this means, in order of increasing energy, first orbital s type, second orbital p type, third orbital d type, fourth orbital s type (denoted as s′) and fifth orbital f type. This input scheme is shown in figure 3 and compared with the experimental single-electron spectrum. We assume a tip/dot/substrate DBTJ with one-dimensional barriers; the dot/substrate barrier is kept constant and the tip–dot barrier can be varied, imitating the experimental conditions. At each electrochemical potential of the tip (in a wide range of potentials) the state transitions in a quantum dot are considered and the corresponding current is calculated by using a stochastic sequence of resonant tunnelling steps; in this way the I–V relationship can be simulated. We simulated tunnelling spectra for different tip–dot distances, and thus different $\Gamma_s^{in}/\Gamma_s^{out}$ ratios. For high $\Gamma_s^{in}/\Gamma_s^{out}$ ratios, the dot can be occupied with more than one electron, giving rise to electron–electron Coulomb interactions. If the Coulomb energies are of the same order of magnitude as the level spacing, the spectra can become very complex. The Monte Carlo simulations were used to assign the peaks in the experimental tunnelling spectra. The spectrum shown in figure 4 (top) was recorded at a tip–dot distance such that $\Gamma_s^{in}/\Gamma_s^{out} \approx 1$. The first peak at positive bias, peak A, corresponds to resonant tunnelling from the tip into the empty s-type LUMO, followed by tunnelling to the substrate electrode:

$$s^0p^0 \xrightarrow{\Gamma_s^{in}} s^1p^0. \tag{2}$$

Tunnelling from the tip into the empty s orbital occurs at an electrochemical potential given by $\mu_e[s^0p^0/s^1p^0] = \varepsilon_s + \Sigma_s$, in which ε_s is the energy of the s level, and Σ_s the polarization energy (charging energy) due to a single electron occupying an s orbital in the CdSe dot [16]. Peak B corresponds to tunnelling from the tip into the s-type orbital, already occupied by one electron:

$$s^1p^0 \xrightarrow{\Gamma_s^{in}} s^2p^0; \tag{3}$$

this step takes place at an electrochemical potential given by $\mu_e[s^1p^0/s^2p^0] = \varepsilon_s + \Sigma_s + J_{s-s}$, in which J_{s-s} is the Coulomb interaction energy of the two electrons in the s orbital [17]. The energy difference between the second and first peaks is thus J_{s-s}, here equal to 75 meV. The second peak is considerably smaller than the first, due to the non-zero probability of finding the s orbital empty at $\mu_e[s^1p^0/s^2p^0]$. The simulations show that peak C corresponds to resonant tunnelling from the tip into the p orbital in an empty quantum dot:

$$s^0p^0 \xrightarrow{\Gamma_p^{in}} s^0p^1. \tag{4}$$

We take into account that the electron in the p level can tunnel to the substrate, or relax to the empty s level, depending on the relative rates of p-to-substrate tunnelling and internal p → s relaxation in the dot. This tunnelling process takes place at $\mu_e[s^0p^0/s^0p^1] = \varepsilon_p + \Sigma_p$. Peak D corresponds to tunnelling into the p orbital, while the s orbital is doubly occupied,

$$s^2p^0 \xrightarrow{\Gamma_p^{in}} s^2p^1 \tag{5}$$

occurring at an electrochemical potential $\mu_e[s^2p^0/s^2p^1] = \varepsilon_p + \Sigma_p + 2J_{s-p}$, where J_{s-p} is the electron–electron Coulomb interaction between an electron in the S and P orbitals. The energy difference between peaks C and D is thus $2J_{s-p}$. Peak E corresponds to tunnelling from the tip to the *third* electron orbital (a d level) while there are two electrons in the quantum dot in the s orbital,

$$s^2d^0 \xrightarrow{\Gamma_p^{in}} s^2d^1; \tag{6}$$

this occurs at an electrochemical potential $\mu_e[s^2p^0d^0/s^2p^0d^1] = \varepsilon_d + \Sigma_d + 2J_{s-d}$. Small satellites are observed together with peak E, reflecting (at much lower probabilities) resonant tunnelling from the tip into the d level while there are more than two electrons present in the quantum dot.

Analysis of a number of tunnelling spectra obtained with different 43 Å CdSe dots shows that J_{s-s} and J_{s-p} are equal to 60 ± 5 meV (corrected for $V_{tip/dot}/V = 0.84$). Pseudo-potential calculations give $J_{s-s} = 280$, 180 and 80 meV and $2J_{s-p} = 550$, 350 and 130 meV for a dielectric constant of the surroundings of 2, 4 and 20 [14]. It should be remarked here that Klein *et al* [1] also found an unexpectedly small value of 15 meV for the hole–hole interaction energy in a 55 Å CdSe quantum dot, mounted via alkanedithiols between two gold electrodes. Most likely, the Coulomb repulsion energy

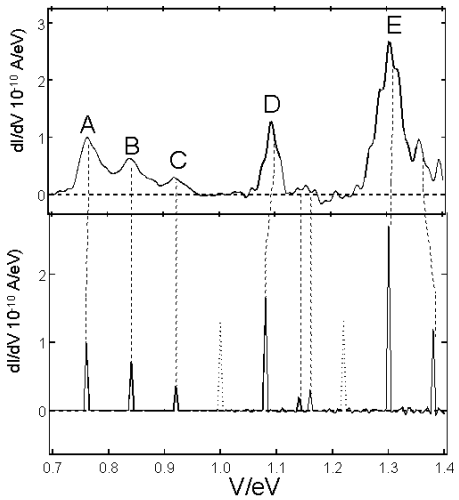

Figure 4. (Top) Spectrum of a 43 Å CdSe quantum dot in the positive bias range obtained with a smaller tip–dot distance than in figure 2; setpoint 60×10^{-12} A at a bias of 1.4 eV; estimated tip–dot distance is 8 Å. (Bottom) Monte Carlo (MC) simulation for $\Gamma_s^{in}/\Gamma_s^{out} = 1$ performed at the single-electron spectrum obtained from pseudo-potential calculations. Details of the MC simulation are reported in [22]. The conductance peaks that have a counterpart in the experimental spectrum are drawn in full, whereas the dashed curves represent peaks that were not found in the upper spectrum.

between two electrons (or holes) is strongly screened. Our results suggest that the dielectric constant of the immediate environment of the dot is effectively increased by the near metal electrode (the platinum tip is at <1 nm from the dot).

It should be noted that two peaks in the simulated spectrum have no complementary peak in the experimental spectrum. These missing peaks correspond to tunnelling through the p and d levels, respectively, while the s orbital is filled with one electron. The origin of the absence of these peaks is not clear yet.

In conclusion, we have analysed resonant tunnelling spectra obtained with an STM probing 43 Å CdSe quantum dots attached to a gold substrate covered with a rigid cyclohexylidene SAM of 8 Å width. We showed that the electron–electron Coulomb interactions in the dot have an important effect on the tunnelling spectra. The probability of these interactions showing up depends sensitively on the relative rates of tunnelling into and out of the CdSe dot. By retracting the tip sufficiently far from the dot, electrons tunnel one at a time through the orbitals of the quantum dot. The corresponding shell-tunnelling spectra show the quasi-particle gap and the energy separations between the first five electron orbitals of the CdSe quantum dot. There is generally a good agreement with the single-electron energy-level spectrum calculated with pseudo-potential theory. By bringing the tip close enough to the dot, multiple occupation of the dot occurs, and shell-filling spectra are observed; these are drastically different from the shell-tunnelling spectrum due to the electron–electron Coulomb interactions.

References

[1] Klein D L, Roth R, Lim A K L, Alivisatos A P and McEuen P L 1997 *Nature* **389** 699–701
[2] Postma H W C, Teepen T, Yao Z, Grifoni M and Dekker C 2001 *Science* **293** 76
[3] Peng Z A and Peng X 2001 *J. Am. Chem. Soc.* **123** 183
[4] Peng X, Schlamp M C, Kadavanich A V and Alivisatos A P 1997 *J. Am. Chem. Soc.* **119** 7019
[5] Su B, Goldman V J and Cunningham J E 1992 *Phys. Rev.* B **46** 7644–55
[6] Williamson A J and Zunger A 2000 *Phys. Rev.* B **61** 1978–91
[7] Franceschetti A and Zunger A 2000 *Phys. Rev.* B **62** 2614–23
[8] Wang L-W and Zunger A 1996 *Phys. Rev.* B **53** 9579–82
[9] Niquet Y M, Allan G, Delerue C and Lannoo M 2000 *Appl. Phys. Lett.* **77** 1182–4
[10] Niquet Y M, Delerue C, Allan G and Lannoo M 2000 *Phys. Rev.* B **62** 5109–16
[11] Micic O I, Jones K M, Cahill A and Nozik A J 1998 *J. Phys. Chem.* B **102** 9791–6
[12] Norris D J and Bawendi M G 1996 *Phys. Rev.* B **53** 16 338–46
[13] Tarucha S, Austing D G, Honda T, van der Hage R J and Kouwenhoven L P 1996 *Phys. Rev. Lett.* **77** 3613–16
[14] Bakkers E P A M, Hens Z, Zunger A, Franceschetti A, Kouwenhoven L P and Vanmaekelbergh D 2001 *Nano. Lett.* **1** 551
[15] Bakkers E P A M and Vanmaekelbergh D 2000 *Phys. Rev.* B **62** R7743–6
[16] Averin D V, Korotkov A N and Likharev K K 1991 *Phys. Rev.* B **44** 6199–211
[17] Franceschetti A, Williamson A and Zunger A 2000 *J. Phys. Chem.* B **104** 3398–401
[18] Banin U, Cao Y, Katz D and Millo O 1999 *Nature* **400** 542–4
[19] Millo O, Katz D, Cao Y and Banin U 2000 *Phys. Rev.* B **61** 16 773–7
[20] Murray C B, Norris D J and Bawendi M G 1993 *J. Am. Chem. Soc.* **115** 8706–15
[21] Bakkers E P A M, Marsman A W, Jenneskens L W and Vanmaekelbergh D 2000 *Angew. Chem., Int. Edn Engl.* **39** 2297–9
[22] Hens Z, Bakkers E P A M and Vanmaekelbergh D 2002 *Phys. Rev.* B submitted